Extended Abstracts of the 2000 International Conference on Solid State Devices and Materials, Sendai, 2000, pp. 94–95

C-2-6

1.55 μm Spot-Size Converter Integrated Laser Diodes Fabricated by Selective Area MOVPE Growth with Various Mask Patterns

Hyun-Soo Kim[1, 2], Dae Kon Oh[2], Moon-Ho Park[2], Nam Hwang[2], and In-Hoon Choi[1]
[1]Department of Materials Science and Engineering, Korea University, Sungbuk-gu, Seoul 132-701, Korea
Phone: +82-2-3290-3705 Fax: +82-2-928-8466 e-mail: kimhyunsoo@hanmail.net
[2]Electronics and Telecommunications Research Institute,
Yusong P.O.Box 106, Taejon 305-600, Korea

1. Introduction

For the laser diodes (LDs) in optical access networks, high coupling efficiency to a single-mode fiber (SMF) or planar lightwave circuit (PLC) is required to reduce the cost of the optical transmitter modules. A conventional semiconductor laser suffers from high coupling loss with a SMF because optical semiconductor devices generally use tightly confined waveguides that maintain a small (1 ~ 2 μm), elliptical mode field, whereas standard SMFs have a relatively large (8 ~10 μm), circular mode field [1]. Recently, spot-size converter integrated LD (SSC-LD) offers the possibility of direct coupling between the semiconductor laser and the SMF without using micro-lens or tapered fibers.

There have been several reports on SSC-LD such as the etched tapered width waveguide [2], the butt-jointed tapered thickness waveguide [3] and the selectively grown tapered thickness waveguide [4]. The last one makes it possible not only to grow the active and passive waveguides simultaneously, but also to control the waveguide thickness variation of the taper by changing the mask pattern. Although 1.3 μm SSC-LD was fabricated by using various techniques [3-8], there are few papers reporting 1.55 μm InGaAs/InGaAsP MQW SSC-LD by using one-step selective area MOVPE.

In this paper, we reported 1.55 μm SSC-LD with vertically tapered waveguide by using various mask patterns. The MQW active and passive waveguide were simultaneously selectively grown by low pressure MOCVD.

2. Device structure and fabrication

Figure 1 shows the various mask patterns for the selective area MOVPE growth. As shown in Fig. 1, in order to investigate the influence of the tapered waveguide structure on the optical far field pattern (FFP), five kinds of tapered waveguides were prepared by varying the mask pattern used for selective area MOVPE. The device structure of the SSC-LD is shown in Fig. 2. The MQW active layer and vertically tapered thickness waveguide were grown simultaneously using various tapered shape masks. The SSC-LD was fabricated using three-step MOCVD.

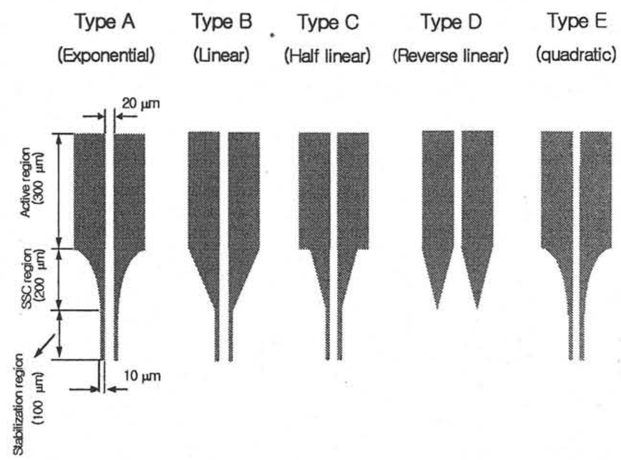

Fig. 1. Various mask patterns for the selective area MOVPE growth

The active layer and tapered thickness waveguide were grown simultaneously by selective area growth. The MQW active layer consists of five pairs of 35 Å-thick InGaAs quantum well and 100 Å-thick lattice-matched InGaAsP barrier (λ_g=1.32 μm) surrounded by 500 Å-thick InGaAsP (λ_g=1.25 μm) separated confinement heterostructure (SCH) layer. After a mesa structure was formed, the second growth step for current blocking was accomplished by growing three layers of p-InP (N_d= $7\times10^{17}cm^{-3}$), n-InP (N_a= $2\times10^{18}cm^{-3}$), and p-InP (N_d= $7\times10^{17}cm^{-3}$). A 2 μm-thick p-InP cladding layer (N_d=$1\times10^{18}cm^{-3}$) and a 0.2 μm-thick p-InGaAs ohmic layer were grown in third growth. The LD section and the SSC section were 300 μm and 300 μm, respectively.

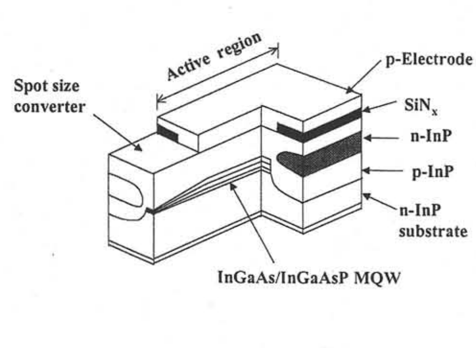

Fig. 2. Schematic diagram of SSC-LD

3. Results and Discussion

Figure 3 shows the growth enhancement ratio (ratio of thickness at the center of the mask opening to the unmasked region) profile along the longitudinal direction for various mask patterns. The high growth enhancement ratio of about 3.0 at the center of the LD active region is obtained. The PL wavelength of MQW layer was changed from 1.55 μm band to 1.3 μm band with a wavelength shift of about 240 nm through the LD active region to the spot size converter region (not shown here). This is suited to reduce the absorption loss of the LD, since the bandgap energy difference between the LD active region and the SSC region is sufficiently large. A typical threshold current is in the range of 25 ~ 35 mA at room temperature except of type D. The type D did not operate. This result could be explained by the large mode conversion loss and large amount of unguided light, because type D have a relatively large slope at the SSC region as shown in Fig. 3.

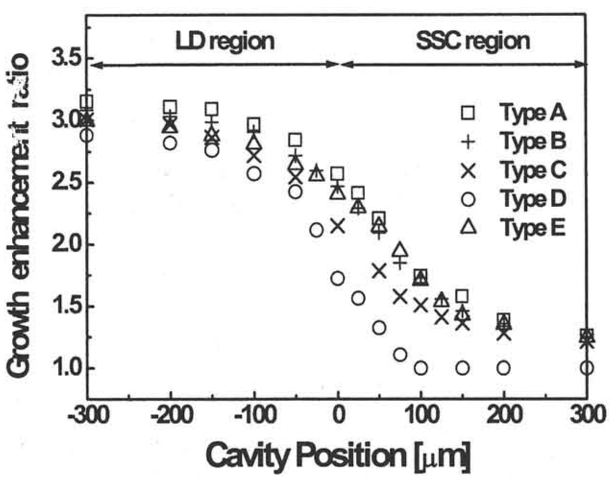

Fig. 3. Growth enhancement ratio (ratio of thickness at the center of the mask opening to the unmasked region) profile along the longitudinal direction for various mask patterns.

Figure 4 shows the measured far-field pattern (FFP) angles for the various SSC-LDs. The typical FFP angle in the vertical direction is in the range of 12 ~ 13°, which is little dependent on mask pattern. On the other hand, The FFP angle in the horizontal direction is in the range of 6.4 ~13.3°, which is more dependent on mask pattern compared to that in the vertical direction. As shown in Fig. 4, the narrowest divergence angle (6.4° × 12.4) was obtained in Type A. The optical coupling characteristics between the flat-ended SMF (single mode fiber) and SSC-LD are shown in figure 5(a) and (b). The minimum coupling loss was as low as 2.76 dB, and the 1-dB alignment tolerances were ±2.4 μm for the horizontal direction, ±2.0 μm for the vertical direction, and 13 μm for the longitudinal direction. Further improvements are expected by the use of a higher barrier (to prevent carrier spillover into the SCH region) and thicker p-InP cladding layers (to avoid adsorption loss by the p-InGaAs contact layer).

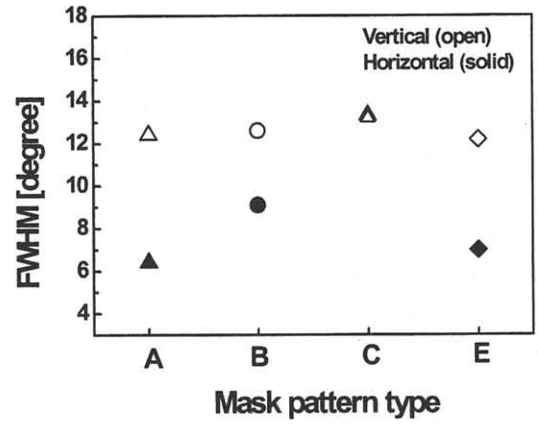

Fig. 4. Far-field pattern angles for various SSC-LDs.

4. Conclusion

We have fabricated SSC-LDs by using selective area MOVPE growth. A narrow divergence angle of 6.4° × 12.4 (horizontal × vertical) was obtained by optimizing the tapered waveguide structure. The minimum coupling loss was as low as 2.76 dB, and the 1-dB alignment tolerances were ±2.4 μm for the horizontal direction, ±2.0 μm for the vertical direction, and 13 μm for the longitudinal direction.

References

[1] O. Mitomi, K. Kasaya, Y. Tohmori, Y. Suzaki, H. Fukano, Y. Sasaki, M. Okamoto and S. Matsumoto, J. Lightwave Technol. **14**, 1714 (1996).

[2] J. R. Kim, J. S. Lee, S. S. Park, M. W. Park, J. S. Yu, S. D. Lee, A. G. Choo and T. I. Kim, J. Korean Phys. Soc. **34**, S281 (1999).

[3] R. Ben-Michael, U.Koren, B. I. Miller, M. G. Young, M. Chien and G. Raybon, IEEE Photon. Technol. Lett. **6**, 1412 (1994).

[4] Y. Suzaki, O. Mitomi, Y. Kondo, Y. Sakai, Y. Kawaguchi, Y. Tohmori, Y. Kadota and M. Yamamoto, J. Lightwave. Technol. **15**, 1602 (1997).

[5] Y. Tohmori, Y. Suzaki, H. Ohashi, Y. Sasaki, Y. Kondo, H. Okamoto, M. Ookamoto, Y. Kadota, O. Mitomi, Y. Itaya and T. Sugie, Electron. Lett. **31**, 1838 (1995).

[6] T. Takiguchi, T. Itagaki, Mo. Takemi, A. Takemoto, T. Miyazaki, K. Shibata, Y. Hisa, K. Goto, Y. Mihashi, S. Takamiya and M. Aiga, J. Crystal Growth **170**, 705 (1997).

[7] Y. Furushima, H. Yamazaki, K. Kudo, Y. Sakata, Y. Okunuki, Y. Sasaki and T. Sasaki, Jpn. J. Appl. Phys **38**, 1234 (1999).

[8] T. J. Kim, J. K. Ji, Y. C. Keh, H. S. Kim, S. D. Lee, A. G. Choo and T. I. Kim, J. Korean Phys. Soc. **34**, S315 (1999).